Title

Carbon declines along tropical forest edges correspond to heterogeneous effects on canopy structure and function

Journal

Proceedings of the National Academy of Sciences of the United States of America, 117(14)

ISSN

0027-8424

Authors

Ordway, Elsa M
Asner, Gregory P

Publication Date

2020-04-07

DOI

10.1073/pnas.1914420117

Carbon declines along tropical forest edges correspond to heterogeneous effects on canopy structure and function

Elsa M. Ordway[a,b,c,1] and Gregory P. Asner[c,1]

[a]Department of Organismic and Evolutionary Biology, Harvard University, Cambridge, MA 02138; [b]Department of Earth System Science, Stanford University, Stanford, CA 94305; and [c]Center for Global Discovery and Conservation Science, Arizona State University, Tempe, AZ 85281

Contributed by Gregory P. Asner, February 7, 2020 (sent for review September 4, 2019; reviewed by David F. R. P. Burslem, Rebecca Chaplin-Kramer, and Nick M. Haddad)

Nearly 20% of tropical forests are within 100 m of a nonforest edge, a consequence of rapid deforestation for agriculture. Despite widespread conversion, roughly 1.2 billion ha of tropical forest remain, constituting the largest terrestrial component of the global carbon budget. Effects of deforestation on carbon dynamics in remnant forests, and spatial variation in underlying changes in structure and function at the plant scale, remain highly uncertain. Using airborne imaging spectroscopy and light detection and ranging (LiDAR) data, we mapped and quantified changes in forest structure and foliar characteristics along forest/oil palm boundaries in Malaysian Borneo to understand spatial and temporal variation in the influence of edges on aboveground carbon and associated changes in ecosystem structure and function. We uncovered declines in aboveground carbon averaging 22% along edges that extended over 100 m into the forest. Aboveground carbon losses were correlated with significant reductions in canopy height and leaf mass per area and increased foliar phosphorus, three plant traits related to light capture and growth. Carbon declines amplified with edge age. Our results indicate that carbon losses along forest edges can arise from multiple, distinct effects on canopy structure and function that vary with edge age and environmental conditions, pointing to a need for consideration of differences in ecosystem sensitivity when developing land-use and conservation strategies. Our findings reveal that, although edge effects on ecosystem structure and function vary, forests neighboring agricultural plantations are consistently vulnerable to long-lasting negative effects on fundamental ecosystem characteristics controlling primary productivity and carbon storage.

Borneo | carbon conservation | forest edge effects | deforestation | leaf traits

Roughly half of the world's forests are within 500 m of a forest edge (1), including the nearly 20% of remaining tropical forest that is now less than 100 m from an edge (1, 2). These remnant tropical forests constitute the largest terrestrial component of the global carbon (C) budget, accounting for 50% of the C stored in global vegetation (350 to 600 gigaton [Gt] C) (3–5). Recent evidence suggests, however, that tropical forests may have transitioned from a net C sink to a net source, emitting 0.43 ± 0.09 Gt C·y^{-1} as a result of widespread deforestation and degradation (6). Edge effects contribute substantially to declines in forest C stocks globally. Using course-resolution MODIS data, Chaplin-Kramer et al. (7) found a 25% reduction in aboveground biomass (AGB) within the first 500 m of forest edges. Similar findings attributed 10.3 Gt of C emissions to edge effects, totaling roughly 31% of estimated annual C emissions due to deforestation in the tropics (2).

Yet tropical forests vary enormously in function, species composition, and turnover rates. This heterogeneity impedes our understanding of the impacts of deforestation on carbon dynamics across the 1.2 billion ha of remaining tropical forests, particularly with respect to underlying changes in structure and function that occur at the tree scale. Given landscape-scale biophysical and topographic variability, the ecological consequences of edge effects on plant-scale structure and function can only be comprehensively understood at organismic resolutions across large spatial scales (8). Evaluating edge effects across forests that differ in function, composition, environmental condition, and level of degradation can provide key insights into how effects vary.

Topography, geology, and associated patterns of nutrient availability influence vegetation patterns at landscape scales. The resulting heterogeneity in forest ecosystems may yield differences in sensitivity or vulnerability to environmental changes following edge creation. Heterogeneous soil nutrient availability across the tropics, reflected in canopy leaf traits associated with nutrient concentrations and photosynthetic capacity (9–11), contributes to variation in net primary productivity and C assimilation at local scales. In addition, tropical forest canopy structure can vary substantially, affecting forest micrometeorological conditions and light environments. Closed-canopy forests generally buffer daily temperature fluctuations and wind and radiation exposure (12). Topography also affects forest micrometeorological conditions by generating distinct microclimatic conditions along hillslopes of different inclination and orientation, potentially influencing forest sensitivity to edge effects at multiple spatial scales. Microclimatic changes that result from edge creation have been shown to differ

Significance

Tropical forests constitute the largest terrestrial component of the global carbon budget. However, rapid agricultural expansion has left these landscapes highly fragmented, calling into question their capacity to cycle and store carbon. We utilized airborne mapping approaches that revealed changes in aboveground carbon and key aspects of ecosystem structure and function in forest edges along oil palm plantations in Malaysian Borneo. We found widespread evidence of significant changes in canopy structure and foliar traits related to light capture, growth, and productivity along forest edges that corresponded to declines in aboveground carbon. These changes underpin carbon declines that varied spatially, with far-reaching implications for the conservation of forest biodiversity and carbon stocks.

Author contributions: E.M.O. and G.P.A. designed research; E.M.O. and G.P.A. performed research; G.P.A. contributed new reagents/analytic tools; E.M.O. analyzed data; and E.M.O. wrote the paper.

Reviewers: D.F.R.P.B., University of Aberdeen; R.C.-K., Stanford University; and N.M.H., Michigan State University.

Competing interest statement: G.P.A. and D.F.R.P.B. are coauthors on several recent papers. They do not collaborate directly.

[1]To whom correspondence may be addressed. Email: elsa.ordway@gmail.com or gregasner@asu.edu.

This article contains supporting information online at https://www.pnas.org/lookup/suppl/doi:10.1073/pnas.1914420117/-/DCSupplemental.

First published March 30, 2020.

spatially and temporally (1, 13, 14), although controls over this variation are poorly understood.

Declines in biomass along forest edges can result from changes to several aspects of ecosystem structure and function. Following the creation of an edge, sunlight and wind penetrate forests laterally, resulting in higher air temperatures, increased vapor-pressure deficit (VPD), and lower soil moisture and relative humidity (13, 15). Forest structure—often characterized by features such as canopy height, stem density, and gap dynamics—is ultimately affected by increased treefall and crown damage. Because aboveground carbon density is a direct function of forest structure, along with wood density, it follows logically that changes to structure will result in changes to aboveground biomass.

In addition to effects on structure, edges can alter ecosystem functions that influence carbon flux dynamics. For example, exacerbated crown damage and treefall along edges can result in larger and more frequent canopy gaps, with effects persisting more than a century after edge creation (16). Greater light penetration to the understory following gap creation alters a light-limited system. Substantial variation in plant functional traits underpins tree species' differing responses to increased light availability. Gaps along edges can thus potentially lead to species composition shifts toward early-successional, light-demanding species over time. As a result, canopy gaps play an important role in tropical forest ecosystems, facilitating succession and contributing to diversity in floristic composition (17). Ultimately, long-term changes to ecosystem structure and function following edge creation can include persistent alterations to gap-phase dynamics, plant community turnover, disrupted seedling recruitment patterns, changes to animal distributions, and altered nutrient and water cycling [e.g., (1, 14–16)].

Here we employ airborne remote-sensing data to examine dynamics in canopy structure and foliar functional traits along edges in large (>5,000 ha) high-diversity remnant forests of Sabah, Malaysian Borneo, an area that has undergone widespread deforestation for oil palm over the last several decades (Fig. 1 and *SI Appendix*, Tables S1 and S2). Our investigation spans a range of topoedaphic conditions, disturbance levels, and edge ages. Using high-fidelity imaging spectroscopy (HiFIS) and light detection and ranging (LiDAR) data from Global Airborne Observatory-3 [GAO; formerly the Carnegie Airborne Observatory (18)], we mapped and quantified changes in forest structure and foliar characteristics related to carbon assimilation, growth strategies, and turnover along the edges of oil palm plantations. We evaluated effects at intact and logged forest sites and utilized site-level average standing biomass as an indicator of logging degradation. We ask: 1) Are edge effects on aboveground carbon consistent across tropical forests that vary in composition, topography, substrate, and level of degradation? 2) What key aspects of canopy structure and function covary with declines in carbon? 3) What additional factors influence how much carbon is lost along a tropical forest edge (i.e., abiotic conditions and time) and how far into a forest do these effects persist? To address these questions, we quantified how aboveground carbon density (ACD; Mg C·ha^{-1}), top-of-canopy height (m), canopy gap frequency (number of gaps per hectare), total canopy gap area (m^2·ha^{-1}), leaf mass per area (LMA; g dry mass [DM] per square meter), and crown-level mass-based foliar nitrogen (N; %) and phosphorus (P; %) vary as a function of distance to edge.

Results and Discussion

Edge Effects on Aboveground Carbon Vary Spatially. Major variation in ACD was observed across the study region, with site-level mean ACD ranging from 50 to 220 Mg C·ha^{-1}. Edge age at each site varied from 2 to roughly 43 y. Despite very recent edge creation in some cases, all sites (n = 27) exhibited significant ($P < 0.01$) declines in ACD as a function of distance from forest edge (Fig. 2). However, both the distance of effect (m) and magnitude (percent change) of these declines varied across sites (*Changepoint Detection*, Fig. 1*B*, and *SI Appendix*, Fig. S1). ACD was 22% lower on average along forest edges, ranging from declines of 16 to 30%, consistent with the 25% decrease in

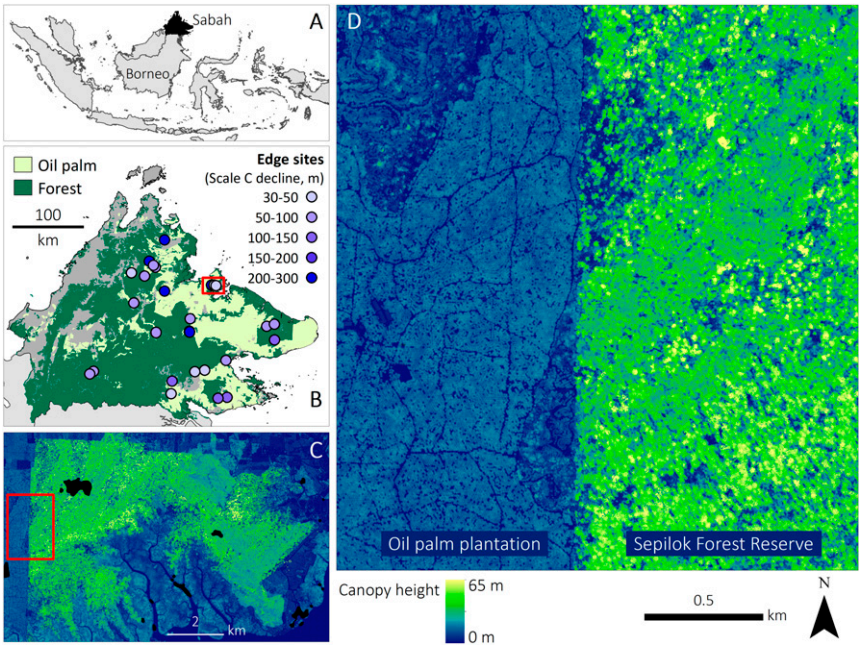

Fig. 1. Study region in Malaysian Borneo where oil palm expansion has resulted in widespread edge creation. (*A*) Study region in Sabah, Malaysian Borneo. (*B*) Sites where edge effects were analyzed are shown as open circles (n = 27). The point color represents the scale over which edge effects on aboveground carbon stocks persisted into the forest in meters, quantified using a changepoint analysis. (*C* and *D*) Canopy height in and around Sepilok Forest Reserve, which contains three of the edge sites studied, illustrating the stark contrast between oil palm plantations (blue) bordering Sepilok and the taller, heterogeneous forest canopy within the reserve.

biomass estimated by Chaplin-Kramer et al. (7). Across Sabah, carbon declines persisted for an average of 114 m into forest interiors before tapering off, which is in line with findings from field-based studies in the Neotropics (19). However, distances varied from 35 m to nearly 300 m. We did not observe significant differences in either the distance or the magnitude of edge effects on ACD between logged and intact forests (Fig. 3).

Carbon Losses Driven by Effects on Leaf Traits and Canopy Height. Broadly similar trends in suppressed ACD along forest edges, indicative of a shift in ecosystem processes, corresponded to distinct changes in canopy structure and leaf traits (Fig. 4 and *SI Appendix*, Table S3). Similar to ACD, we conducted independent changepoint detection analyses of each variable as a function of distance to the forest edge to identify the distance and magnitude of effects across sites (*Methods*). Canopy height was significantly lower at forest edges, with varying effects on leaf traits and gap dynamics. Edge effects on canopy height and foliar traits persisted over distances that were comparable to ACD declines averaging 64 to 92 m, although there was considerable variation (*SI Appendix*, Table S3). LMA generally decreased at forest edges, while foliar P and N increased. The frequency and area of canopy gaps increased measurably at forest edges at less than 40% of the sites. See *SI Appendix*, *Results* for a detailed description of edge effects on structure and function.

To explore what ecosystem changes were the most dominant force on ACD declines, we conducted a principal-component regression evaluating coordination between edge effects on canopy height, gaps, and foliar traits. The principal-component analysis revealed two main axes of edge effects corresponding to canopy structural damage (gaps) and plant traits (LMA, foliar P, and canopy height; *SI Appendix*, Table S4). We found no significant relationship between the magnitude of declines in ACD and variation in the magnitude of edge effects on these other key aspects of ecosystem function. However, the principal-component axes capturing variance in the distance of edge effects on structural damage and traits explained over half of the variation in the distance of ACD declines ($r = 0.57$, $P = 0.0002$), with the relationship driven by a positive correlation with the trait axis ($r = 0.52$, $P < 0.0001$).

Sites spanned the two principal-component axes depending on how coupled or decoupled edge effects were on structure and function (*SI Appendix*, Fig. S3). For example, sites at one end of the trait axis exhibited tightly coupled effects on LMA and P and reduced canopy height, which contrasted with sites where edges affected only a single trait or the scale and magnitude of effects on traits differed. The varying scale of ACD declines emerged from these site-level differences in effects on structure and function.

Edge Age, Topography, and Substrate Mediate Effects. We explored what site-level differences influenced edge effects on ACD and canopy structure and function, focusing on variation in edge age (time since edge creation), topography (elevation, slope, and topographic position index; TPI), edaphic conditions (dominant soil type), and forest degradation (average standing biomass) (*Methods*). Variation in the magnitude of ACD decline was correlated with edge age and soil type (adjusted $R^2 = 0.42$, $P = 0.016$, normalized root-mean-square error [RMSE] = 3.15%). Edge effects amplified with time, evidenced by a noisy but significant increase in the magnitude of ACD declines with edge age (adjusted $R^2 = 0.30$, $P = 0.006$; Fig. 5). Large declines observed at sites with edges that were over 40 y old indicate that effects on ACD can persist for decades. This finding corresponds to previous studies showing that tropical forest edges require only 10 to 50 y to reach a new, postdisturbance equilibrium (20, 21). Still, a longer time series may be necessary to understand whether aboveground carbon stocks along forest edges will begin to regenerate or remain equilibrated at a new stable state across sites with such a broad range of abiotic factors. Surprisingly, we found no evidence of ACD declines receding further into the forest over time as described by Gascon et al. (15).

The only canopy structure or foliar variable that changed significantly with time was foliar P (adjusted $R^2 = 0.22$, $P = 0.03$). The magnitude of increased P became more pronounced with increasing edge age until leveling off after ~20 y (*SI Appendix*, Fig. S4). Additionally, we found that topography influenced the coupling of edge effects on foliar traits and canopy height, even

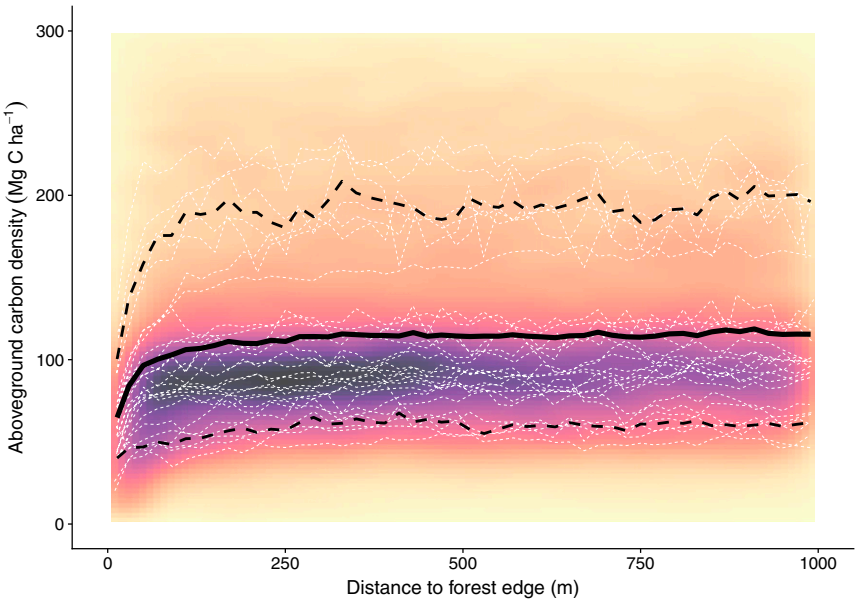

Fig. 2. Declines in aboveground carbon at forest edge. White dashed lines show changes in aboveground carbon density (Mg C·ha^{-1}) for all 27 edge sites. The average decline across all sites is illustrated by the solid black line (black dashed lines show the 10th and 90th percentiles). Colors illustrate a 2D kernel density plot of all ACD observations at all sites (n = 158,736). Darker colors indicate more observations.

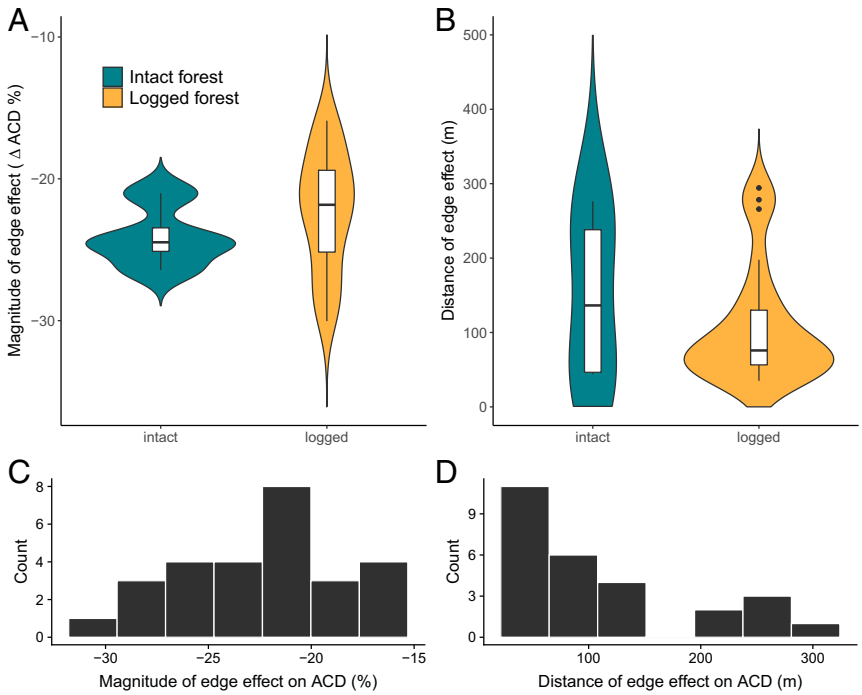

Fig. 3. Heterogeneous declines in carbon. Declines in ACD varied across sites in terms of both the magnitude (*A* and *C*) and distance (*B* and *D*) of the edge effect. No significant difference was observed between logged ($n = 4$) and intact ($n = 23$) sites.

after controlling for elevation prior to quantifying edge effects. Sites with similar magnitudes of effects on leaf traits and canopy height were generally at locations with a lower TPI ($R^2 = 0.26$, $P = 0.01$) and lower slopes ($R^2 = 0.18$, $P = 0.04$). Sites where the scale of edge effects on leaf traits and canopy height were highly coupled typically occurred in areas with lower slopes ($R^2 = 0.48$, $P = 0.0003$), a lower TPI ($R^2 = 0.44$, $P = 0.0005$), and at lower elevations ($R^2 = 0.29$, $P = 0.008$). Soil type was the only variable significantly correlated with the distance of ACD declines (adjusted $R^2 = 0.31$, $P = 0.03$, RMSE = 60.65). Sites on Gleyic Acrisol/Luvisol soils (Silabukan Association in Sabah) were correlated with ACD declines that persisted over greater distances.

In combination, these results reveal that the spatial scale of ACD loss was strongly correlated with the scale of edge effects on other aspects of ecosystem function (canopy height, LMA, foliar P, and gaps) which varied with topography (slope, TPI, and elevation), mediated by soil type. Topography and edaphic conditions are known to be important drivers of structure, function, and composition in Sabah's lowland tropical forests (22–26). Our findings provide evidence that the underlying composition, structure, and edaphic characteristics of forests across the region further contribute to variation in their responses to edge dynamics.

As an example, two sites with ACD declines that persisted for some of the largest distances in this study occurred in low-lying areas on Silabukan (Gleyic Acrisol/Luvisol) soils, immediately adjacent to compositionally and structurally distinct forests on relatively steeper slopes with Lokan soils (Orthic Acrisols). Large, slow-growing dipterocarps (e.g., *Shorea multiflora*) are more common on nutrient-poor Lokan soils that exhibit low concentrations of N, P, and base cations (22). In contrast, higher-fertility alluvial forests on Silabukan soils have greater tree species diversity (23), dominated by tall, fast-growing dipterocarps [e.g., *Parashorea tomentella* (22)]. Alluvial forests are more susceptible to mortality due to the combination of fast-growing dipterocarps with lower wood densities on more saturated soils that limit root development, resulting in higher turnover rates and primary production than forests on Lokan soils. The increased gap area and frequency observed along alluvial forest edges are consistent with increased susceptibility to crown damage and mortality imposed by environmental conditions (27).

Processes Underpinning Aboveground Carbon Declines. Our findings across edaphically and topographically contrasting conditions suggest that multiple, distinct processes result in observed carbon declines. Specifically, we show that edges significantly affect canopy structure as well as LMA and foliar P—key leaf traits related to light capture, growth, longevity, and defense (28–30). Here, we explore mechanisms that could drive variation in observed edge effects across sites as they relate to altered gap-phase dynamics, microclimatic conditions, and human impact.

In addition to directly reducing canopy height and lowering biomass, larger and more frequent canopy gaps along forest edges drive increased light availability. Regeneration quickly sets in, fostering regrowth of both pioneer species (found in gaps and early-successional forests) and shade-tolerant species (found in undisturbed areas) (31). If pioneer species dominate recovery processes, this compositional shift results in an increase in the abundance of fast-growing species along edges, generally exhibiting lower LMA and higher foliar nutrient concentrations. Where gap frequency and area were greater along edges, we observed significant declines in LMA, consistent with expectations. Surprisingly, however, we only observed significant edge effects on canopy gap dynamics at 39% of the sites, suggesting that declines in ACD were more often driven by canopy height reductions associated with shifting ecosystem processes rather than altered gap-phase dynamics.

At over half of the sites, where we found a lack of measurable edge effect on canopy gaps, observed changes in foliar traits may reflect plant responses to altered microclimatic conditions that arise purely from light, wind, and warmer temperatures penetrating the forest laterally over short distances. High temperatures and desiccation have been observed in logged forests and oil palm plantations in Borneo, supporting this potential explanation

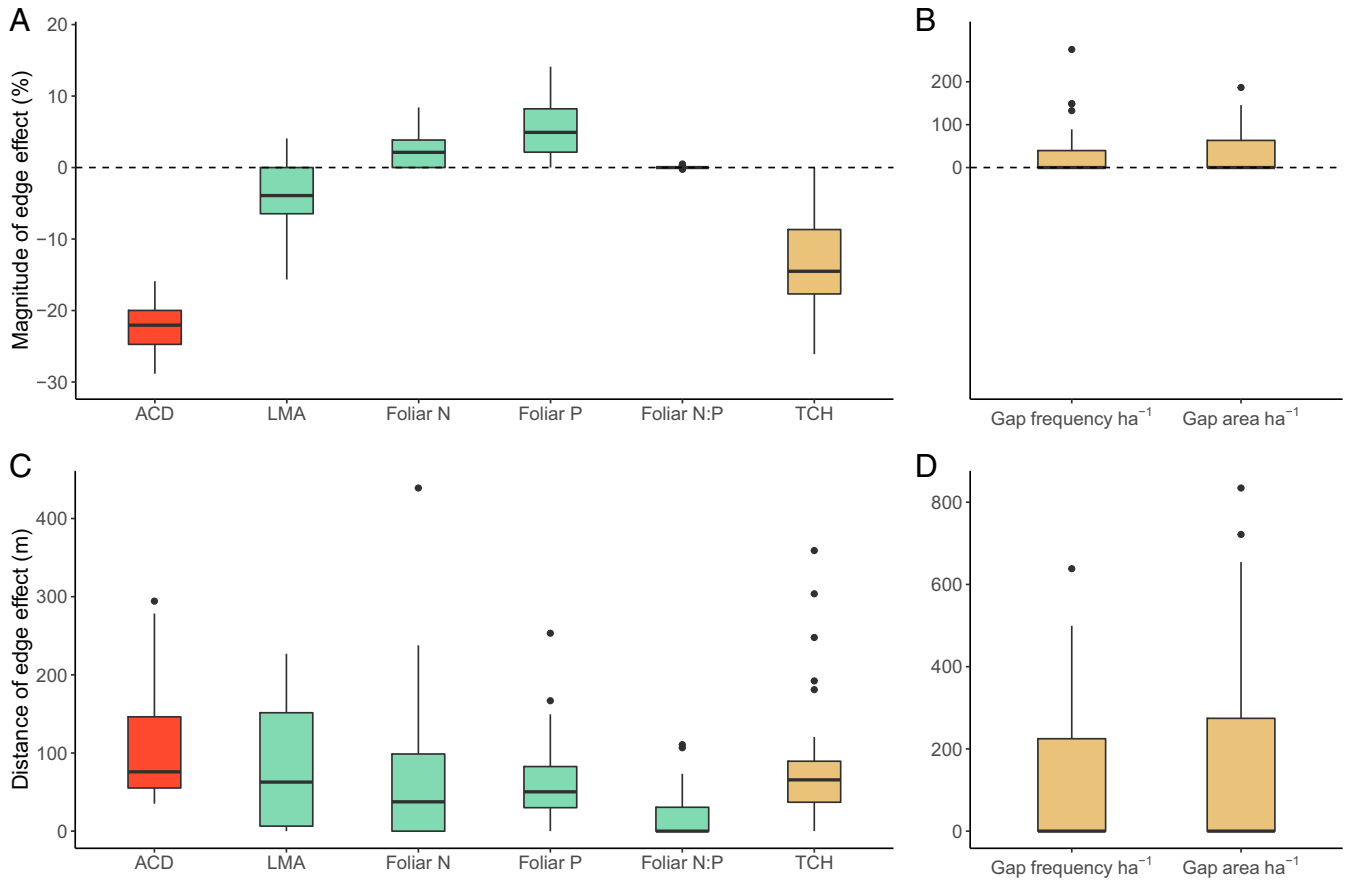

Fig. 4. (*A* and *B*) Declines in ACD (red) along forest edges were observed at all sites alongside significant but heterogeneous effects on foliar traits (green) and canopy structure (yellow). (*C* and *D*) The distance over which declines in ACD persisted corresponded to edge effects on foliar traits and canopy height. Effects on ACD, foliar traits, and canopy height were observed within the first 100 to 200 m of a forest edge, while measurable effects on canopy gaps persisted for several hundred meters. TCH, top-of-canopy height.

(32, 33). During the warmest period of the day, oil palm plantations in Borneo can be 6.5 °C warmer than closed-canopy, old-growth forest, exhibiting increased soil temperatures and VPD (32). Increases in air temperature and VPD, lower soil moisture and relative humidity, and higher wind speeds result in drought-like conditions along forest edges, stressing plants and leading to leaf abscission and increased litterfall (34). These changes affect nutrient cycles, altering foliar nutrient concentrations and productivity. The ACD losses associated with strong changes in LMA and foliar P, even in the absence of altered gap dynamics, is indicative of a lateral microclimate-driven decline in carbon (*SI Appendix*, Fig. S3).

Interestingly, we observed a strong coupling of foliar P concentrations and LMA to edge conditions, despite limited effects on foliar N. This aligns, however, with known nutrient limitations in Southeast Asian forests. Strong P limitations in Bornean dipterocarp forests [e.g., (18)] make soil fertility a stronger driver of changes in LMA and foliar P than foliar N (35). Results from a fertilization experiment similarly demonstrate that elevated foliar P concentrations observed in this study could arise from either elevated N or P concentrations in soils following increased abscission and litterfall due to laterally driven microclimate changes (36). In addition to nutrient conditions, LMA also responds to changes in light, with shade-intolerant species (e.g., pioneers) displaying higher plasticity in response to light (37).

Although a decline in ACD associated with increased nutrient concentrations may seem counterintuitive, it is consistent with observed relationships between productivity, AGB, turnover rate, and nutrient availability. Forest growth rates in the Amazon have been shown to be significantly correlated with soil P content (38). Forests on younger, more fertile soils in the western Amazon support higher rates of biomass productivity but lower AGB than forests on older, nutrient-poor soils in the central Amazon and Guiana Shield. This difference is largely correlated with higher stem turnover on nutrient-rich soils resulting in higher productivity but lower stored aboveground biomass (38, 39). Similarly, Qie et al. (40) found declines in AGB along forest edges in Borneo associated with higher turnover accompanied by significant declines in stand-level wood density, suggestive of a community composition shift toward more fast-growing species that accumulate less biomass.

Lastly, we were unable to explain a large amount of the variation in the magnitude of ACD declines. The remaining unexplained variance could be associated with several variables that we were unable to quantify or adequately account for. These include the method of edge creation (e.g., mechanical clearing or fire), hunting pressure, or changes in animal behavior along oil palm edges which could influence seed dispersal [e.g., (41)], and fuelwood collection, illegal logging, and small-scale timber harvesting that could result in anthropogenically driven declines in aboveground carbon. We visually assessed each edge included in the study using high-resolution LiDAR data and Google Earth imagery to exclude all sites where oil palm plantations or large-scale logging concessions were actively expanding into forest areas. However, the acute boundary between oil palm plantations and forests across Sabah (Fig. 1) makes these areas considerably

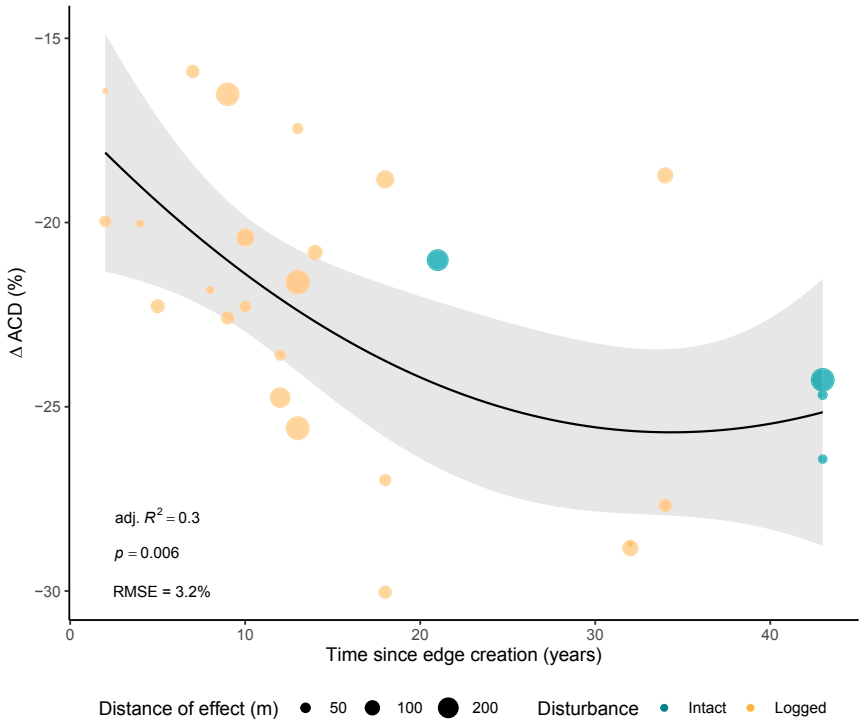

Fig. 5. Relationship between percent declines in aboveground carbon density (ΔACD) and edge age at all edges in the study, including intact (blue circles) and logged (yellow circles) forest sites. The distance over which ACD declines persisted at each site is indicated by the circle size. Shaded areas around the line correspond to predicted mean likelihood 95% CIs calculated using SEs from the modeled quadratic relationship between ΔACD and edge age across all forest edge sites (n = 27).

more accessible to people, heightening the potential exposure of forest edges to hunting pressure and illegal logging. We would expect selective timber removal from illegal logging to result in increased canopy gap area and frequency, which occurred at fewer than 40% of the edges in this study. We also found no relationship between the distance or magnitude of ACD declines and site-level standing biomass, a measure of degradation associated with logging intensity. However, with our dataset, we are unable to rule out the possibility that people played a role in observed edge effects.

Conservation and Management Implications. Looking beyond areas of active land-use change, this study reveals that forest conversion to monoculture oil palm plantations imparts long-lasting effects on forest structure and function that extend past cropland boundaries, into remnant forests. These effects were evident at sites where edges were present for only 2 y and for over 4 decades. Consequently, tropical forests set aside for conservation or left uncleared are still affected by the conversion of adjacent landscapes and are vulnerable to changes in ecosystem characteristics that control primary productivity and carbon storage. Our finding that edge effects become more severe with time underscores a need for a management response. Furthermore, carbon accounting and reporting that neglect these impacts will underestimate carbon losses, which has major implications considering nearly 20% of remaining tropical forests lie within 100 m of a forest edge (1, 2). One possible strategy for mitigating edge-related declines in aboveground carbon and human encroachment across these boundaries is to create buffer zones (e.g., timber plantations) between cropland and forest ecosystems.

Critically, our results indicate that spatial variation in processes underpinning declines in aboveground carbon along cropland/forest edges arises from several distinct changes in canopy structure and function corresponding to edge age, forest composition, and environmental variation, making some forests more vulnerable to edge effects than others. Further research on this topic would benefit from inclusion of a larger number of sites across different tropical forest regions to evaluate how edge effects covary in time with species composition, topography, and environmental conditions. In lieu of such research, our findings point to a need for careful consideration of the spatial variation in ecosystem sensitivity to edge creation across tropical forests when developing land-use planning and conservation strategies.

Methods

Study Area. As of 2016, remaining natural forests covered 59% of Sabah, Malaysian Borneo, roughly 3.7 million ha (Mha) (42). Oil palm and timber plantations, which account for 1.8 Mha, extend directly to the perimeter of most of these remnant forests, resulting in a highly fragmented landscape (Fig. 1). Fragment size below a certain threshold (roughly 2,000 to 4,000 ha) can influence the severity of edge effects (43). This study focused on edges along large remnant forest stands (>5,000 ha) bordered by oil palm plantations. We restricted our analysis to lowland forests (<700 m) and flight-line locations that encompassed forest areas ≥250 ha along oil palm edges on a single substrate. We excluded mangroves and peat swamp forests. The median edge length across sites was 1,927 m, ranging from 477 to 9,403 m.

Forest Structure and Foliar Characteristics. We examined eight forest structure variables and foliar characteristics that are strongly linked to ecosystem function and have demonstrated measurability with high accuracy using airborne remote-sensing techniques (*SI Appendix*, Table S2). In addition to aboveground carbon density, we analyzed edge effects on leaf mass per area, foliar nitrogen and phosphorus concentrations, foliar N:P ratios, canopy height, and gap dynamics. In tropical forests, gaps in the canopy caused by the death of one or more trees are the dominant form of disturbance. Increased light availability, in the otherwise light-limited understory, can lead to changes in seedling recruitment and competition, nutrient cycling, and species composition (44, 45). Greater wind penetration and desiccation along forest edges have been shown to result in larger and more frequent gaps associated with the mortality of large trees, which can substantially influence canopy height and biomass (46, 47).

Foliar N, P, and LMA control photosynthesis, primary production, and plant responses to microclimatic changes (48). The uptake of N and P is required for light capture and C fixation. Although tropical forests are relatively

N-abundant, insufficient available P constrains ecosystem processes, including primary productivity (49, 50). Foliar N:P ratios indicate limitation by P or N, with values >16 suggestive of P limitation and values <14 suggestive of N limitation at the community level (51). N:P ratios in tropical forests are not well-constrained, however, and are highly responsive to environmental and phylogenetic controls (52).

LMA is a key indicator of plant growth strategies, covarying strongly with foliar N and P (29). At the slow-return end of the leaf economics spectrum, plants in poor-nutrient conditions with low foliar nutrient concentrations invest more in leaf structure and defense, expressed as high LMA, strategizing longer-lived, more durable leaves with slower decomposition rates at the expense of slower growth. At the quick-return end of the spectrum, plants in nutrient-rich environments with higher foliar nutrient concentrations invest less in structure and defense, enabling faster growth in a more rapid foliar turnover environment (via abscission and herbivory). This latter growth strategy supports higher photosynthetic rates and more rapid C gain (29). LMA is phylogenetically constrained (53), although it can also vary strongly with light and temperature changes and moderately under nutrient- and water-stressed conditions (37). Shade-intolerant species have been found to display higher LMA plasticity in their response to light relative to shade-tolerant species (37, 54).

Airborne Remote-Sensing Data. To measure forest structure and foliar characteristics, we used coaligned LiDAR and HiFIS data collected by the GAO in April 2016 using the Airborne Taxonomic Mapping System (18). LiDAR data were collected at a minimum pulse density of 1.14 pulses per square meter and processed to top-of-canopy height (m) at a 2-m ground-level resolution using the LAStools software suite (Rapidlasso). Aboveground carbon density (Mg C·ha^{-1}) at 30-m ground-level resolution was estimated using top-of-canopy height and gap equations from Jucker et al. (55), described in Asner et al. (42). Static gaps in the forest canopy (present during the time of the GAO data collection) were measured according to the definition put forth by Brokaw (56). Brokaw defines gaps as openings in the forest canopy that extend down to an average height of ≤2 m above the forest floor (56). Canopy gaps were identified using 2-m ground-level-resolution canopy height data. A filter was used to exclude gaps of less than 4 pixels. Gap frequency (number of gaps per hectare) and total gap area (m^2·ha^{-1}) were calculated on a per-hectare basis.

HiFIS data were collected at 4-m ground-level resolution using a visible to shortwave imaging spectrometer that measures spectral radiance in 427 channels at 5-nm bandwidths from 350 to 2,485 nm. After averaging the radiance data to 10-nm bands, ACORN-6LX atmospheric correction software was used to transform the HiFIS radiance data to apparent surface reflectance (Imspec). Each study site was processed through ACORN using mean flight conditions (elevation, collection altitude, sensor and solar view angles, and time) specific to that site. Crown-level foliar chemical traits and LMA were estimated by linking spectral observations with field-based measurements of foliar characteristics (57, 58), summarized here. Individual trees identified as visible within the HiFIS reflectance data were sampled across 13 field locations in Sabah. Mature top-of-canopy leaf samples were collected from at least two fully sunlit branches of each tree. Leaf samples were scanned, weighed, and dried for at least 72 h before dry mass was measured. Leaf mass per area was calculated as g DM·m^{-2}. Detailed descriptions of chemical analysis protocols, standards, and instruments used to extract total element concentrations of N and P are described in refs. 53, 59, and 60.

To ensure accurate comparison between laboratory measurements of N, P, and LMA and the corresponding airborne spectroscopy data, the spectral data were restricted to well-lit portions of tree crowns. After applying a hand-generated cloud and cloud-shadow mask, spectral data were filtered based on a 2-m-height requirement to exclude bare ground and nonforest vegetation, and a normalized difference vegetation index threshold of ≥0.75 to ensure sufficient foliar cover for pixels included. Spectral bands in the 440- to 1,320-, 1,500- to 1,760-, and 2,040- to 2,440-nm wavelengths were omitted due to high atmospheric water absorption. Filtered spectral data were brightness-normalized to eliminate anomalously low or high reflectance values.

A partial least-squares regression model was generated to relate the brightness-normalized surface reflectance spectra to laboratory-assayed foliar traits across the state of Sabah, Malaysia, and this model was subsequently applied across surface reflectance imagery to generate foliar trait maps. Crown-level mass-based foliar N (%) and P (%) concentrations and LMA values were predicted with R^2 = 0.54, 0.65, and 0.81 and RMSE = 0.43, 0.03, and 23.90 (58). The mapped foliar traits were used to calculate foliar N:P ratios across the Sepilok study area. N:P ratios are broadly used to infer the potential limitation of N or P with respect to primary productivity (51, 61). Low N:P values, less than circa 14, are considered to indicate N limitation, while values >16 indicate P limitation (52).

Changepoint Detection. To identify whether forest structure and foliar characteristics significantly varied near forest edges, we conducted a changepoint analysis (*SI Appendix*, Fig. S5). Changepoint detection, also known as structural change or breakpoint analysis, is an algorithmic approach using maximum-likelihood estimation to quantify the point at which the statistical properties of a sequence of observations change (62). Analyses were carried out for each variable across the entire dataset at each edge site.

Two approaches were compared to identify whether there was a significant edge effect and, if so, the distance of that effect (i.e., the changepoint location where the effect asymptotes, measured as a function of distance to forest edge). A piecewise linear model consisting of two linear segments was used to identify a single changepoint. Multiple changepoints were detected using a nonlinear asymptotic model, $y = a - be^{-cx}$, where x is distance from the forest edge and y is the variable of interest. If multiple statistically significant changepoints were detected, the changepoint that most accurately represented a visible change in trend in the data was selected. Changepoints were considered significant at $P < 0.01$ and compared with an intercept-only model based on Akaike's information criterion.

We limited analyses to within ≤2,000 m of the forest edge for ACD, canopy height, and gap metrics, and to within ≤1,000 m for foliar chemical traits and LMA. These distances were selected based on a large body of literature citing that 99% of all documented effects occur within 2 km of a forest edge, and within tens of meters of an edge in the case of the latter variables (14, 15). Four of the 27 edge sites lacked sufficient HiFIS data at forest–oil palm edges (*SI Appendix*, Table S1, sites 2, 6, 10, and 13), reducing foliar N, foliar P, and LMA changepoint analyses to 23 sites. We conducted changepoint analyses using mean values as a function of a distance to an edge for ACD, canopy height, and foliar chemical traits, which were normally distributed. Because gap frequency and gap area had skewed distributions, however, we conducted changepoint analyses using the median values for both gap metrics.

In the case of LMA and foliar N and P, we attempted to control for elevation using a method employed by Chadwick and Asner (11) by fitting a second-order polynomial and dividing the residuals by the 2nd to 98th percentile range for each trait prior to conducting the changepoint analysis. For foliar N and P, we additionally controlled for LMA to remove the statistical artifact of LMA driving any observed edge effect relationship. Elevation derived from the GAO LiDAR data was used to control for elevation. All analyses were implemented in R using the raster, changepoint, and SiZer packages (63–66).

Edge Effect Variation. To explore what factors best explained variation in edge effects on ACD, canopy structure, and canopy function, we employed forward, backward, and best subset selection. We focused on differences in edge age (time since edge creation), topography (elevation, slope, and topographic position index), edaphic conditions (dominant soil type), and forest degradation (average standing biomass). We visually assessed time series of Google Earth and Landsat image collections to identify the date of edge creation at each location. These archives collectively date back to 1972. Slope and TPI were calculated from the GAO LiDAR-derived elevation data. The model with the minimum necessary parameters that explained the greatest amount of variation in the magnitude of decline in ACD was identified by selecting the model with the lowest Bayesian information criterion (BIC). The most parsimonious model included edge age (quadratic fit) and dominant soil type (adjusted R^2 = 0.42, P = 0.016, RMSE = 3.15%), although edge age resulted in the strongest relationship (adjusted R^2 = 0.30, P = 0.006; Fig. 5). Edge age and dominant soil type were included in the lowest BIC model of the distance of ACD declines using forward and best subset selection (adjusted R^2 = 0.32, P = 0.048, RMSE = 56.92 m). Backward selection only included soil type, which accounted for most of the variation in the combined model (adjusted R^2 = 0.31, P = 0.03, RMSE = 60.65).

Principal-Component Regression. To explore what ecosystem changes were the most dominant force on ACD declines, we conducted a principal-component analysis (PCA) evaluating coordination between edge effects on canopy height, structural damage (gaps), and foliar traits. Analyses were restricted to 23 sites with sufficient foliar trait data. We conducted one PCA based on the distance of edge effects for foliar N and P, LMA, canopy height, gap frequency, and gap area (*SI Appendix*, Fig. S3*A*). A second PCA analyzed the magnitude of the edge effect for these same six variables (*SI Appendix*, Fig. S3*B*). The PC1 and PC2 axis scores were then correlated with the distance effect on ACD (*SI Appendix*, Fig. S3*A*) or the magnitude of the edge effect on ACD (*SI Appendix*, Fig. S3*B*).

Data Availability Statement. All data used in analyses presented in the paper are provided in *SI Appendix*. Datasets S1–S6 include data and metadata on aboveground carbon density, elevation, mass-based foliar nitrogen concentrations, mass-based foliar phosphorus concentrations, canopy gap frequency, total canopy gap area,

leaf mass per area, top-of-canopy height, the site location corresponding to *SI Appendix*, Table S1, and the distance of each observation from the forest-oil palm edge. See Dataset S1 for metadata information.

ACKNOWLEDGMENTS. We thank N. Vaughn, P. Brodrick, R. Martin, U. Jami, I. Karolus, and others in the Arizona State University field team for supporting underpinning aspects of this work. We thank our partners from the Sabah Forestry Department, South East Asia Rainforest Research Partnership, Partners of Community Organizations in Sabah (PACOS) Trust, Layang Layang Aerospace, and other organizations within Malaysia for their support of this study. Airborne mapping, processing, and analysis were funded by the United Nations Development Programme Global Environment Facility, Avatar Alliance Foundation, Roundtable on Sustainable Palm Oil, Worldwide Fund for Nature, Morgan Family Foundation, and Rainforest Trust. E.M.O. was supported by the NSF Graduate Research Fellowship Program (Grant 2012118590) and by a postdoctoral fellowship from the Harvard University Center for the Environment. The Global Airborne Observatory has been made possible by grants and donations to G.P.A. from the Avatar Alliance Foundation; Margaret A. Cargill Foundation; David and Lucile Packard Foundation; Gordon and Betty Moore Foundation; Grantham Foundation for the Protection of the Environment; W. M. Keck Foundation; John D. and Catherine T. MacArthur Foundation; Andrew Mellon Foundation; Mary Anne Nyburg Baker and G. Leonard Baker Jr.; and William R. Hearst III.

1. N. M. Haddad *et al*., Habitat fragmentation and its lasting impact on Earth's ecosystems. *Sci. Adv.* **1**, e1500052 (2015).
2. K. Brinck *et al*., High resolution analysis of tropical forest fragmentation and its impact on the global carbon cycle. *Nat. Commun.* **8**, 14855 (2017).
3. G. B. Bonan, Forests and climate change: Forcings, feedbacks, and the climate benefits of forests. *Science* **320**, 1444–1449 (2008).
4. R. A. Houghton, F. Hall, S. J. Goetz, Importance of biomass in the global carbon cycle. *J. Geophys. Res.* **114**, G00E03 (2009).
5. Y. Pan *et al*., A large and persistent carbon sink in the world's forests. *Science* **333**, 988–993 (2011).
6. A. Baccini *et al*., Tropical forests are a net carbon source based on aboveground measurements of gain and loss. *Science* **358**, 230–234 (2017).
7. R. Chaplin-Kramer *et al*., Degradation in carbon stocks near tropical forest edges. *Nat. Commun.* **6**, 10158 (2015).
8. Y. Malhi, T. A. Gardner, G. R. Goldsmith, M. R. Silman, P. Zelazowski, Tropical forests in the Anthropocene. *Annu. Rev. Environ. Resour.* **39**, 125–159 (2014).
9. V. Maire *et al*., Global effects of soil and climate on leaf photosynthetic traits and rates. *Glob. Ecol. Biogeogr.* **24**, 706–717 (2015).
10. G. P. Asner *et al*., Landscape biogeochemistry reflected in shifting distributions of chemical traits in the Amazon forest canopy. *Nat. Geosci.* **8**, 567 (2015).
11. K. D. Chadwick, G. P. Asner, Landscape evolution and nutrient rejuvenation reflected in Amazon forest canopy chemistry. *Ecol. Lett.* **21**, 978–988 (2018).
12. H. G. Jones, *Plants and Microclimate: A Quantitative Approach to Environmental Plant Physiology* (Cambridge University Press, Cambridge, UK, 2013).
13. S. M. Gehlhausen, M. W. Schwartz, C. K. Augspurger, Vegetation and microclimatic edge effects in two mixed-mesophytic forest fragments. *Plant Ecol.* **147**, 21–35 (2000).
14. E. N. Broadbent *et al*., Forest fragmentation and edge effects from deforestation and selective logging in the Brazilian Amazon. *Biol. Conserv.* **141**, 1745–1757 (2008).
15. C. Gascon, G. B. Williamson, G. A. da Fonseca, Ecology. Receding forest edges and vanishing reserves. *Science* **288**, 1356–1358 (2000).
16. N. R. Vaughn, G. P. Asner, C. P. Giardina, Centennial impacts of fragmentation on the canopy structure of tropical montane forest. *Ecol. Appl.* **24**, 1638–1650 (2014).
17. M. D. Swaine, T. C. Whitmore, On the definition of ecological species groups in tropical rain forests. *Vegetatio* **75**, 81–86 (1988).
18. G. P. Asner *et al*., Carnegie Airborne Observatory-2: Increasing science data dimensionality via high-fidelity multi-sensor fusion. *Remote Sens. Environ.* **124**, 454–465 (2012).
19. W. F. Laurance *et al*., Ecosystem decay of Amazonian forest fragments: A 22-year investigation. *Conserv. Biol.* **16**, 605–618 (2002).
20. W. F. Laurance, S. G. Laurance, P. Delamonica, Tropical forest fragmentation and greenhouse gas emissions. *For. Ecol. Manage.* **110**, 173–180 (1998).
21. S. Pütz, J. Groeneveld, L. F. Alves, J. P. Metzger, A. Huth, Fragmentation drives tropical forest fragments to early successional states: A modelling study for Brazilian Atlantic forests. *Ecol. Modell.* **222**, 1986–1997 (2011).
22. J. E. D. Fox, *A Handbook to Kabili-Sepilok Forest Reserve* (Sabah Forest Record, Borneo Literature Bureau for Sabah Forest Department, Sabah, Malaysia, 1973), No. 9.
23. R. Nilus, "Effect of edaphic variation on forest structure, dynamics, diversity and regeneration in a lowland tropical rain forest in Borneo," Dissertation, University of Aberdeen, Aberdeen, UK (2004).
24. D. H. Dent, D. F. Burslem, Performance trade-offs driven by morphological plasticity contribute to habitat specialization of Bornean tree species. *Biotropica* **41**, 424–434 (2009).
25. D. H. Dent, D. F. Burslem, Leaf traits of dipterocarp species with contrasting distributions across a gradient of nutrient and light availability. *Plant Ecol. Divers.* **9**, 521–533 (2016).
26. T. Jucker *et al*., Topography shapes the structure, composition and function of tropical forest landscapes. *Ecol. Lett.* **21**, 989–1000 (2018).
27. E. M. Everham, N. V. Brokaw, Forest damage and recovery from catastrophic wind. *Bot. Rev.* **62**, 113–185 (1996).
28. P. B. Reich, J. Oleksyn, Global patterns of plant leaf N and P in relation to temperature and latitude. *Proc. Natl. Acad. Sci. U.S.A.* **101**, 11001–11006 (2004).
29. I. J. Wright *et al*., The worldwide leaf economics spectrum. *Nature* **428**, 821–827 (2004).
30. P. B. Reich, The world-wide 'fast–slow' plant economics spectrum: A traits manifesto. *J. Ecol.* **102**, 275–301 (2014).
31. N. V. Brokaw, Gap-phase regeneration in a tropical forest. *Ecology* **66**, 682–687 (1985).
32. S. R. Hardwick *et al*., The relationship between leaf area index and microclimate in tropical forest and oil palm plantation: Forest disturbance drives changes in microclimate. *Agric. Meteorol.* **201**, 187–195 (2015).
33. B. Blonder *et al*., Extreme and highly heterogeneous microclimates in selectively logged tropical forests. *Front. Forests Glob. Change* **1**, 5 (2018).
34. P. M. Brando *et al*., Prolonged tropical forest degradation due to compounding disturbances: Implications for CO_2 and H_2O fluxes. *Glob. Change Biol.* **25**, 2855–2868 (2019).
35. G. D. Paoli, Divergent leaf traits among congeneric tropical trees with contrasting habitat associations on Borneo. *J. Trop. Ecol.* **22**, 397–408 (2006).
36. E. Mirmanto, J. Proctor, J. Green, L. Nagy, Suriantata, Effects of nitrogen and phosphorus fertilization in a lowland evergreen rainforest. *Philos. Trans. R. Soc. Lond. B Biol. Sci.* **354**, 1825–1829 (1999).
37. H. Poorter, U. Niinemets, L. Poorter, I. J. Wright, R. Villar, Causes and consequences of variation in leaf mass per area (LMA): A meta-analysis. *New Phytol.* **182**, 565–588 (2009).
38. C. A. Quesada *et al*., Basin-wide variations in Amazon forest structure and function are mediated by both soils and climate. *Biogeosciences* **9**, 2203–2246 (2012).
39. C. Baraloto *et al*., Disentangling stand and environmental correlates of aboveground biomass in Amazonian forests. *Glob. Change Biol.* **17**, 2677–2688 (2011).
40. L. Qie *et al*., Long-term carbon sink in Borneo's forests halted by drought and vulnerable to edge effects. *Nat. Commun.* **8**, 1966 (2017).
41. P. S. Ashton, "Dipterocarpaceae" in *Tree Flora of Sabah and Sarawak*, E. Soepadmo, L. G. Saw, R. C. K. Chung, Eds. (Forest Research Institute Malaysia/Sabah Forestry Department/Sarawak Forestry Department, 2004), vol. 5, pp. 63–388.
42. G. P. Asner *et al*., Mapped aboveground carbon stocks to advance forest conservation and recovery in Malaysian Borneo. *Biol. Conserv.* **217**, 289–310 (2018).
43. W. F. Laurance, E. Yensen, Predicting the impacts of edge effects in fragmented habits. *Biol. Conserv.* **55**, 77–92 (1991).
44. S. T. A. Pickett, P. S. White, *The Ecology of Natural Disturbance and Patch Dynamics* (Academic Press, Orlando, FL, 1985).
45. S. I. Yamamoto, Forest gap dynamics and tree regeneration. *J. For. Res.* **5**, 223–229 (2000).
46. W. F. Laurance *et al*., The fate of Amazonian forest fragments: A 32-year investigation. *Biol. Conserv.* **144**, 56–67 (2011).
47. G. Briant, V. Gond, S. G. Laurance, Habitat fragmentation and the desiccation of forest canopies: A case study from eastern Amazonia. *Biol. Conserv.* **143**, 2763–2769 (2010).
48. C. Field, H. A. Mooney, "The photosynthesis - nitrogen relationship in wild plants" in *On the Economy of Plant Form and Function*, T. J. Givnish, Ed. (Cambridge University Press, Cambridge, UK, 1986), pp. 25–55.
49. P. M. Vitousek, Litterfall, nutrient cycling, and nutrient limitation in tropical forests. *Ecology* **65**, 285–298 (1984).
50. P. M. Vitousek, S. Porder, B. Z. Houlton, O. A. Chadwick, Terrestrial phosphorus limitation: Mechanisms, implications, and nitrogen-phosphorus interactions. *Ecol. Appl.* **20**, 5–15 (2010).
51. W. Koerselmann, A. F. M. Meuleman, The vegetation N:P ratio: A new tool to detect the nature of nutrient limitation. *J. Appl. Ecol.* **33**, 1441–1450 (1996).
52. A. R. Townsend, C. C. Cleveland, G. P. Asner, M. M. Bustamante, Controls over foliar N:P ratios in tropical rain forests. *Ecology* **88**, 107–118 (2007).
53. G. P. Asner, R. E. Martin, Canopy phylogenetic, chemical and spectral assembly in a lowland Amazonian forest. *New Phytol.* **189**, 999–1012 (2011).
54. F. Valladares, S. J. Wright, E. Lasso, K. Kitajima, R. W. Pearcy, Plastic phenotypic response to light of 16 congeneric shrubs from a Panamanian rainforest. *Ecology* **81**, 1925–1936 (2000).
55. T. Jucker *et al*., Estimating aboveground carbon density and its uncertainty in Borneo's structurally complex tropical forests using airborne laser scanning. *Biogeosciences* **15**, 3811–3830 (2018).
56. N. V. Brokaw, The definition of treefall gap and its effect on measures of forest dynamics. *Biotropica* **14**, 158–160 (1982).
57. K. Chadwick, G. Asner, Organismic-scale remote sensing of canopy foliar traits in lowland tropical forests. *Remote Sens.* **8**, 87 (2016).
58. R. E. Martin *et al*., An approach for foliar trait retrieval from airborne imaging spectroscopy of tropical forests. *Remote Sens.* **10**, 199 (2018).
59. G. P. Asner, R. E. Martin, Spectranomics: Emerging science and conservation opportunities at the interface of biodiversity and remote sensing. *Glob. Ecol. Conserv.* **8**, 212–219 (2016).
60. G. P. Asner *et al*., Amazonian functional diversity from forest canopy chemical assembly. *Proc. Natl. Acad. Sci. U.S.A.* **111**, 5604–5609 (2014).
61. J. T. Tessier, D. J. Raynal, Use of nitrogen to phosphorus ratios in plant tissue as an indicator of nutrient limitation and nitrogen saturation. *J. Appl. Ecol.* **40**, 523–534 (2003).
62. R. Killick, I. Eckley, changepoint: An R package for changepoint analysis. *J. Stat. Softw.* **58**, 1–19 (2014).
63. R. J. Hijmans, raster: Geographic Data Analysis and Modeling. R Package Version 2.5-8. https://CRAN.R-project.org/package=MuMIn. Accessed 17 March 2020.
64. R. Killick, K. Haynes, I. Eckley, P. Fearnhead, J. Lee, changepoint: Methods for Changepoint Detection. R Package Version 2.2.2. https://cran.r-project.org/web/packages/changepoint/changepoint.pdf. Accessed 31 January 2019.
65. R. J. Sonderegger, SiZer: Significant Zero Crossings. R Package Version 0.1-5. https://cran.r-project.org/web/packages/SiZer/SiZer.pdf. Accessed 31 January 2019.
66. R Core Development Team, *R: A Language and Environment for Statistical Computing*. https://www.r-project.org/. Accessed 31 January 2019.